

# DeFlow: Decoupling Manifold Modeling and Value Maximization for Offline Policy Extraction

Zhancun Mu<sup>1</sup>

## Abstract

We present DeFlow, a decoupled offline RL framework that leverages flow matching to faithfully capture complex behavior manifolds. Optimizing generative policies is computationally prohibitive, typically necessitating backpropagation through ODE solvers. We address this by learning a lightweight refinement module within an explicit, data-derived trust region of the flow manifold, rather than sacrificing the iterative generation capability via single-step distillation. This way, we bypass solver differentiation and eliminate the need for balancing loss terms, ensuring stable improvement while fully preserving the flow’s iterative expressivity. Empirically, DeFlow achieves superior performance on the challenging OGBench benchmark and demonstrates efficient offline-to-online adaptation.

<http://muzhancun.github.io/preprints/deflow>

## 1. Introduction

Offline reinforcement learning (RL) fundamentally requires solving two coupled challenges: faithfully modeling the behavior distribution to ensure constraint satisfaction, and maximizing a value function to achieve policy improvement (Levine et al., 2020). As the community moves towards large-scale, multimodal datasets (e.g., OGBench (Park et al., 2025a)), the first challenge, *modeling*, has necessitated the use of highly expressive generative policies, particularly Diffusion Models and Flow Matching (Lipman et al., 2023; Sohl-Dickstein et al., 2015). These iterative models excel at capturing complex, non-Gaussian behavior manifolds that traditional unimodal policies fail to represent.

However, extracting a high-value policy from these generative models presents a stark *expressivity-optimizability*

<sup>1</sup>Peking University, Institute of Artificial Intelligence, China, Beijing. Correspondence to: Zhancun Mu <muzhancun@stu.pku.edu.cn>.

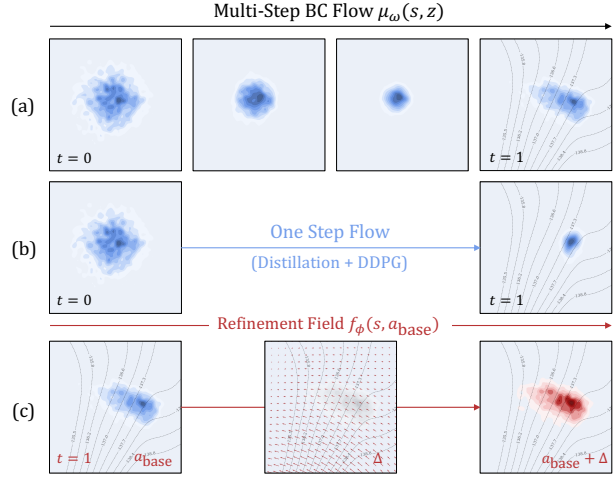


**Figure 1. DeFlow Framework.** (a) **Iterative Flow Prior:** A multi-step flow policy faithfully captures the complex, multimodal structure of the dataset. (b) **The Compression Bottleneck** (e.g., FQL): Existing methods often distill the flow into a one-step policy to enable joint optimization. This compression leads to *expressivity collapse*, failing to cover the manifold. (c) **DeFlow (Ours):** We retain the full expressive power of the iterative flow (Blue) to define the *support*, and decouple the optimization into a lightweight refinement module (Orange). This enables precise value maximization without destroying the manifold geometry.

*dilemma*. Directly optimizing the iterative generation process (solving ODEs/SDEs) for Q-values requires backpropagating through the solver (BPTT), which is computationally prohibitive and numerically unstable. To circumvent this, recent state-of-the-art methods like Flow Q-Learning (FQL) (Park et al., 2025c) attempt to distill the iterative flow into a one-step generator (Figure 1b) to enable tractable joint optimization. We argue that this compression creates a critical *expressivity bottleneck*. By forcing the complex, iterative generation process into a single step, these methods sacrifice the very modeling capacity they sought to achieve, failing to cover the multimodal support of the dataset and resulting in suboptimal, collapsed policies.

In this work, we propose to resolve this dilemma not by compressing the model or modifying the pipeline (Zhang et al., 2025b), but by structurally **decoupling** the objectives.

We introduce **DeFlow**, a framework that assigns the responsibility of *manifold representation* and *policy improvement* to distinct components.

Specifically, DeFlow comprises two distinct components: (1) A **Flow Matching Policy** optimized exclusively via supervised learning to capture the behavior manifold; and (2) A lightweight **Action Refinement Module** that maximizes Q-values via deterministic policy gradients (DDPG (Lillicrap et al., 2016)). Instead of distorting the flow model’s weights to find high rewards, the refinement module learns a residual shift on the generated action (Figure 1c).

A critical challenge in this decoupled setting is preventing the refinement module from drifting off the valid data manifold (Out-of-Distribution actions). We address this via an automated Lagrangian constraint mechanism. Unlike standard regularization which requires fixed, brittle hyperparameters, our Lagrangian multiplier dynamically adjusts the penalty based on the divergence between the refined action and the flow support.

This decoupled design offers three significant advantages over prior joint-optimization methods:

- **Preservation of Manifold Geometry:** By isolating the flow training from Q-learning gradients, DeFlow prevents mode collapse. The flow model provides a stable, high-fidelity anchor, ensuring the policy remains grounded in the dataset support even during aggressive value maximization.
- **Optimization Stability & Efficiency:** DeFlow bypasses the need for computationally expensive BPTT. The refinement module utilizes efficient, standard gradients, making policy extraction significantly faster and more stable.
- **Seamless Offline-to-Online Adaptation:** The Lagrangian mechanism serves as an auto-tuning gate-keeper. During offline training, it tightly constrains the policy to the dataset. During online fine-tuning, as the agent collects new data and the Q-estimates become reliable, the Lagrangian multiplier automatically adjusts, allowing the refinement module to explore more aggressively. This enables DeFlow to adapt online without the need for manual hyperparameter retuning or structural changes.

We evaluate DeFlow on the challenging multimodal tasks of OGBench (Park et al., 2025a) and standard D4RL benchmarks (Fu et al., 2020). Our results demonstrate that decoupling modeling from improvement allows DeFlow to match or outperform state-of-the-art methods that rely on complex joint optimization. DeFlow effectively extracts high-performance policies while maintaining the structural integrity of the learned behavior distribution.

## 2. Preliminaries

We consider the standard Markov Decision Process (MDP) (Puterman, 2014) defined by the tuple  $(\mathcal{S}, \mathcal{A}, r, p, \gamma)$ , where  $\mathcal{S}$  and  $\mathcal{A}$  denote the state and action spaces,  $r(s, a)$  the reward function,  $p(s'|s, a)$  the transition dynamics, and  $\gamma \in [0, 1]$  the discount factor.

### 2.1. Offline RL as Constrained Optimization

In offline RL, we are given a static dataset  $\mathcal{D} = \{(s, a, r, s')\}$  collected by a behavior policy  $\pi_\beta$ . The goal is to learn a policy  $\pi_\theta$  that maximizes the expected cumulative return. However, due to the distributional shift, simply maximizing values on out-of-distribution (OOD) actions leads to extrapolation errors. Thus, offline RL is formally cast as a constrained optimization problem (Levine et al., 2020):

$$\begin{aligned} & \max_{\pi_\theta} \mathbb{E}_{s \sim \mathcal{D}, a \sim \pi_\theta(\cdot|s)} [Q(s, a)] \\ & \text{s.t. } \mathbb{D}(\pi_\theta(\cdot|s) || \pi_\beta(\cdot|s)) \leq \epsilon, \end{aligned} \quad (1)$$

where  $Q(s, a)$  is the state-action value function and  $\mathbb{D}$  is a divergence measure (e.g., KL divergence or Wasserstein distance) ensuring the policy stays within the support of  $\mathcal{D}$ .

**Critic Learning.** To evaluate the policy, we learn a critic  $Q_\phi$  by minimizing the standard Bellman error (Mnih et al., 2013). The objective is:

$$\mathcal{L}_Q(\phi) = \mathbb{E}_{s, a, r, s' \sim \mathcal{D}} \left[ \left( Q_\phi(s, a) - r - \gamma \hat{Q}_{\bar{\phi}}(s', a') \right)^2 \right], \quad (2)$$

where  $a' \sim \pi_\theta(\cdot|s')$  and  $\hat{Q}_{\bar{\phi}}$  utilizes a target network for stability.

**The Actor’s Dilemma.** Standard methods typically convert the constrained problem in Eq. (1) into an unconstrained one via a Lagrangian relaxation with a fixed penalty coefficient  $\alpha$ :

$$\mathcal{L}_\pi(\theta) = \mathbb{E}_{s \sim \mathcal{D}} \left[ -\underbrace{\mathbb{E}_{a \sim \pi_\theta} [Q_\phi(s, a)]}_{\text{DDPG Loss}} + \alpha \cdot \underbrace{\mathcal{L}_{\text{BC}}(\pi_\theta, \mathcal{D})}_{\text{BC Loss}} \right]. \quad (3)$$

Existing approaches face a structural dichotomy here: Gaussian policies allow efficient gradient ascent on the RL Objective (via the reparameterization trick) but fail to minimize  $\mathcal{L}_{\text{BC}}$  for multimodal data. Conversely, generative policies (like Flow Matching) minimize  $\mathcal{L}_{\text{BC}}$  perfectly but make optimizing the RL objective intractable, as differentiating through the sampling chain is computationally prohibitive. Furthermore, treating  $\alpha$  as a static hyperparameter often leads to poor constraint satisfaction across different tasks (Park et al., 2025c; Agrawalla et al., 2025).

## 2.2. Conditional Flow Matching

To address the modeling challenge, we leverage Conditional Flow Matching (CFM) (Lipman et al., 2023), which offers a simulation-free alternative to diffusion training. CFM learns a time-dependent vector field  $v_\psi(t, x) : [0, 1] \times \mathbb{R}^d \rightarrow \mathbb{R}^d$  that pushes a simple prior distribution  $p_0$  (e.g.,  $\mathcal{N}(0, I)$ ) to the data distribution  $p_1$  (e.g.,  $\pi_\beta(a|s)$ ).

The generative process is defined by an Ordinary Differential Equation (ODE):

$$\frac{d}{dt} \Psi_t(x) = v_\psi(t, \Psi_t(x)), \quad \Psi_0(x) = x \sim p_0, \quad (4)$$

where  $\Psi_t$  is the flow map. We adopt the Optimal Transport (OT) path (Lipman et al., 2024), which corresponds to the linear interpolation  $x_t = (1-t)x_0 + tx_1$ . The vector field is trained via the regression objective:

$$\mathcal{L}_{\text{FM}}(\psi) = \mathbb{E}_{t \sim \mathcal{U}[0,1], x_0 \sim p_0, x_1 \sim \mathcal{D}} \|v_\psi(t, x_t) - (x_1 - x_0)\|^2. \quad (5)$$

**Flow as a Policy.** In our context, the flow model serves as a state-conditional generator. We denote the generated action as a deterministic function of the initial noise  $z$  and state  $s$ :

$$a_{\text{flow}} = \text{ODESolve}(v_\psi, s, z), \quad z \sim \mathcal{N}(0, I). \quad (6)$$

Crucially, while this flow model captures the behavior distribution precisely, it acts as a referential manifold in our framework, decoupling the complexity of distribution modeling from the policy improvement step described next.

## 3. DeFlow: Disentangling Fidelity and Optimality

The philosophy underpinning DeFlow is a structural disentanglement of policy learning. We posit that forcing a single generative model to simultaneously master density estimation (Behavior Cloning) and value maximization (RL) creates a competing objective landscape. To resolve this, we propose a functionally decoupled architecture that leverages the strengths of both worlds. Algorithm 1 provides an overview of our method.

We formulate the policy as a composite function, where the final action  $a$  is derived from a **Base Flow**  $\mu_\psi$  adjusted by a **Refinement Module**  $f_\phi$ :

$$a = \underbrace{\text{sg}[\mu_\psi(s, z)]}_{\text{Fixed Proposal}} + f_\phi(s, \underbrace{\text{sg}[\mu_\psi(s, z)]}_{\text{Context}}), \quad z \sim \mathcal{N}(0, I) \quad (7)$$

Here,  $\text{sg}[\cdot]$  denotes the stop-gradient operator. In this paradigm,  $\mu_\psi$  acts as a multi-step flow matching model that faithfully learns the behavior manifold, providing a high-quality ‘‘proposal’’ action. The module  $f_\phi$ , implemented as

### Algorithm 1 DeFlow

```

function  $\mu_\psi(s, z)$  ▷ Base flow policy
  for  $t = 0, 1, \dots, M-1$  do
     $z \leftarrow z + v_\psi(t/M, s, z)/M$  ▷ Euler method
  return  $z$ 

function SAMPLE_ACTION( $s$ )
   $z \sim (0, I_d)$ 
   $a_{\text{base}} \leftarrow \mu_\psi(s, z)$ 
   $a_{\text{refine}} \leftarrow f_\phi(s, a_{\text{base}})$  ▷ Stop gradient
  return  $a_{\text{base}} + a_{\text{refine}}$ 

while not converged do
  Sample batch  $\{(s, a, r, s')\} \sim \mathcal{D}$ 
  ▷ Train critic  $Q$ 
   $z \sim (0, I_d)$ 
   $a' \sim \text{SAMPLE\_ACTION}(s)$ 
  Update  $\phi$  to minimize  $\mathbb{E}[(Q(s, a) - r - \gamma \bar{Q}(s', a'))^2]$ 
  ▷ Train vector field  $v_\psi$  in BC flow policy  $\mu_\psi$ 
   $x^0 \sim \mathcal{N}(0, I_d)$ 
   $x^1 \leftarrow a$ 
   $t \sim \text{Unif}([0, 1])$ 
   $x^t \leftarrow (1-t)x^0 + tx^1$ 
  Update  $\psi$  to minimize  $\mathbb{E}[\|\mu_\psi(t, s, x^t) - (x^1 - x^0)\|_2^2]$ 
  ▷ Train refinement policy  $f_\phi$ 
   $z \sim (0, I_d)$ 
   $a_{\text{base}} \leftarrow \text{STOPGRADIENT}(\mu_\psi(s, z))$ 
   $\Delta \leftarrow f_\phi(s, a_{\text{base}})$ 
  Update  $\phi$  to minimize  $\mathbb{E}[-Q_\phi(s, a_{\text{base}} + \Delta) + \alpha \|\Delta\|_2^2]$ 
  ▷ Train coefficient  $\alpha$ 
  Update  $\alpha$  to minimize  $\mathbb{E}_{s, z}[-\alpha \cdot \text{sg}(\|\Delta a\|^2 - \delta)]$ 
return  $\mu_\psi, f_\phi$ 

```

a lightweight MLP, learns an optimal residual to shift this proposal toward high-value regions.

**The role of Stop-Gradient:** Crucially, the stop-gradient operator cuts the computational graph between the refinement module and the flow model. This implies that during the update of  $f_\phi$ , the base flow  $\mu_\psi$  is treated as a fixed stochastic generator rather than a differentiable layer. This design choice effectively bypasses the need to backpropagate gradients through the ODE solver—a process known to be computationally expensive and numerically unstable—thereby allowing for efficient, distinct optimization loops for both modules.

### 3.1. Revisiting Existing Coupling Paradigms

To better contextualize DeFlow, we briefly analyze the limitations inherent in two prevalent strategies for integrating flow models with Q-learning.

**Paradigm I: End-to-End Policy Steering.** Ideally, one might update a flow model  $\pi_\psi$  by backpropagating the Q-

gradient through the ODE integration chain:

$$\nabla_\psi \mathcal{L}_{\text{RL}} = \mathbb{E}_{s,z} \left[ \frac{\partial Q(s, a)}{\partial a} \cdot \frac{\partial \text{ODESolve}(v_\psi, s, z)}{\partial \psi} \right]. \quad (8)$$

While theoretically elegant, this “steering” approach faces significant practical hurdles. Computing  $\frac{\partial \text{ODESolve}}{\partial \psi}$  necessitates BPTT or the Adjoint Method across numerous integration steps. This is not only memory-intensive but also susceptible to the vanishing gradient problem—similar to training very deep RNNs—which often hinders the policy from effectively navigating towards high-Q regions.

**Paradigm II: Single-step Shortcut Distillation.** Alternatively, methods like FQL (Park et al., 2025c) attempt to bypass the ODE complexity by distilling the iterative flow into a single-step policy  $\pi_\theta(s, z)$ . The actor is typically trained with a composite objective:

$$\mathcal{L}_\pi(\omega) = \underbrace{\mathbb{E}_{s,a^\pi}[-Q_\phi(s, a^\pi)]}_{\text{Q maximization}} + \underbrace{\alpha \mathcal{L}_{\text{Distill}}(\omega)}_{\text{BC regularization}}. \quad (9)$$

While efficient at inference, this paradigm risks an *expressivity collapse*, as the shortcut model may fail to capture the complex, multi-modal distributions represented by the original flow. Furthermore, the scalar  $\alpha$  introduces a sensitive hyperparameter trade-off: a large  $\alpha$  limits improvement, while a small  $\alpha$  leads to manifold deviation.

### 3.2. The DeFlow Approach

DeFlow addresses these challenges by maintaining the *Multi-step Flow* as a foundational anchor while employing a *Residual Refinement* for optimization.

The Base Flow  $\mu_\psi$  is updated solely via the Flow Matching objective  $\mathcal{L}_{\text{FM}}(\psi)$ . This ensures it remains an unbiased estimator of the behavior distribution, undisturbed by the high variance often associated with Q-learning gradients.

Inspired by trust-region methods, we formulate the refinement as a constrained optimization problem. Rather than using a fixed penalty coefficient, we constrain the magnitude of the refinement  $\|\Delta a\|^2$  within a dynamic budget  $\delta$ :

$$\max_{f_\phi} \mathbb{E}_{s,z}[Q(s, a_{\text{flow}} + \Delta a)] \quad \text{s.t.} \quad \mathbb{E}_{s,z}[\|\Delta a\|^2] \leq \delta, \quad (10)$$

where  $\Delta a = f_\phi(s, a_{\text{flow}})$  and  $a_{\text{flow}} = \text{sg}[\mu_\psi(s, z)]$ . The parameter  $\delta$  (target divergence) represents the permissible deviation from the behavior manifold, which can be intuitively set based on the action space scale.

To solve Equation (10), we employ the method of Lagrange multipliers. We first apply **Q-Normalization** to the RL objective to mitigate the scale variance of  $Q$ -values across different environments. We then introduce a learnable Lagrangian multiplier  $\alpha$  (where  $\alpha > 0$ ). The loss function for

#### Remark: Instance-Level vs. Policy-Level Residuals

While residual learning is a well-established concept, it is vital to distinguish **Instance-level Refinement** from traditional **Policy-level Residuals**.

Prior approaches like Silver et al. (2019) typically model the policy as  $\pi_{\text{final}}(s) = \pi_{\text{base}}(s) + \pi_{\text{res}}(s)$ . Here, the residual  $\pi_{\text{res}}$  is strictly *state-dependent*. While effective for unimodal corrections (e.g., sim-to-real dynamics gaps), this formulation is ill-suited for generative policies. Since  $\pi_{\text{base}}$  captures a multimodal distribution (e.g., branching paths), a state-dependent residual applies a uniform vector shift across all modes. This is problematic: a shift that optimizes one mode (e.g., turn left) might be detrimental to another (e.g., turn right).

In contrast, DeFlow computes  $\Delta a = f_\phi(s, a_{\text{base}})$ , explicitly conditioning the residual on the *sampled action instance*. This transforms the residual module from a global bias correction into a *local vector field* on the action manifold. It allows  $f_\phi$  to apply distinct, context-aware adjustments—optimizing a “left turn” sample differently from a “right turn” sample originating from the same state.

the refinement module  $f_\phi$  is defined as:

$$\mathcal{L}_{\text{Refine}}(\phi) = \mathbb{E}_{s,z} \left[ -\frac{Q(s, \text{sg}[a_{\text{flow}}] + \Delta a)}{\text{sg}[\|Q_{\text{mean}}\|]} + \alpha \cdot \|\Delta a\|^2 \right]. \quad (11)$$

Mirroring the automated entropy tuning found in Soft Actor-Critic (SAC) (Haarnoja et al., 2018),  $\alpha$  is automatically adjusted to satisfy the constraint by minimizing:

$$\mathcal{L}(\alpha) = \mathbb{E}_{s,z} [-\alpha \cdot \text{sg}(\|\Delta a\|^2 - \delta)]. \quad (12)$$

This automated constraint mechanism offers distinct advantages:

- **Intuitive Hyperparameters:** Unlike an abstract penalty coefficient which is sensitive to loss scaling,  $\delta$  carries physical significance (squared distance in action space), making it robust and easier to tune.
- **Adaptive Balancing:** The mechanism acts as a feedback controller. If the refinement becomes too aggressive ( $\|\Delta a\|^2 > \delta$ ),  $\alpha$  increases to enforce manifold adherence; conversely, if the policy is conservative,  $\alpha$  decreases to prioritize value maximization.
- **Online Compatibility:** This formulation naturally extends to online fine-tuning, where  $\delta$  can be viewed similarly to target entropy, allowing the policy to dynamically balance the exploration-exploitation trade-off as the Q-function matures.

**Seamless Offline-to-Online (O2O) Adaptation.** Beyond its performance in static datasets, the decoupled nature of DeFlow offers a principled framework for the transition from offline pre-training to online fine-tuning. In the online phase, a notorious challenge is maintaining the integrity of the learned behavioral prior while allowing for further exploration. Under our paradigm, the Base Flow  $\mu_\psi$  can be effectively “frozen” to serve as a high-fidelity manifold anchor, significantly reducing the computational overhead and stabilizing the distribution. Meanwhile, the Refinement Module  $f_\phi$  retains its plasticity, evolving to capture new high-reward regions with the auto-tuned multiplier  $\alpha$ . We provide an extensive evaluation of this O2O flexibility in Section 5.

## 4. Related Works

**Offline RL and Scaling.** The fundamental paradigm of offline RL (Levine et al., 2020) involves learning a value function while constraining the policy to the behavioral distribution to avoid extrapolation errors. Classic approaches implement this via explicit regularization (Kumar et al., 2020; Fujimoto & Gu, 2021) or in-sample maximization (Kostrikov et al., 2022; Xu et al., 2023). However, the recent emergence of large-scale, high-dimensional benchmarks such as OGBench (Park et al., 2025a) has shifted the community’s focus towards *scaling* offline RL. Recent works like Park et al. (2025b;d;e) suggest that simply scaling model parameters is insufficient; instead, there remains significant room for improvement in the fundamental algorithms for both Q-learning and policy extraction to handle complex data distributions effectively.

**Generative Modeling with Flow Matching.** To meet the demand for high-expressivity modeling, the field has increasingly adopted iterative generative models. While earlier works introduced diffusion models for planning (Janner et al., 2022) or data augmentation (Lu et al., 2023a), the current frontier focuses on leveraging *Flow Matching* (FM) (Lipman et al., 2023) to model complex policies and value functions. FM offers a more stable and efficient training objective than diffusion. Consequently, a wave of recent methods has successfully applied FM to both behavior cloning and Q-learning, including FQL (Park et al., 2025c), MeanFlowQL (Wang et al., 2025), SORL (Espinosa-Dice et al., 2025), SAC Flow (Zhang et al., 2025b), floq (Agrawalla et al., 2025), and Value Flows (Dong et al., 2025). These methods treat the Bellman update or policy extraction as a flow matching problem, significantly improving performance on complex tasks.

### 4.1. Policy Optimization with Diffusion and Flow Models

The central challenge in training generative policies for offline RL lies in simultaneously satisfying two conflicting

objectives: *faithfully modeling the behavioral distribution (Constraint)* and *maximizing the value function (Improvement)*. Prior works have explored different trade-offs to address this conflict.

**Gradient Propagation and Weighting.** Early works based on diffusion models sought to inject value information directly into the generation process. One strategy is *Weighted Behavioral Cloning* (e.g., QGPO (Lu et al., 2023b), EDP (Kang et al., 2023), QIPO (Zhang et al., 2025a)), which avoids gradients entirely by simply re-weighting the BC loss using AWR (Peng et al., 2019). While stable, this approach is often sample-inefficient as it discards low-value data. Alternatively, methods like Diffusion-QL (Wang et al., 2023), Consistency-AC (Ding & Jin, 2024) apply *Reparameterized Policy Gradients*, backpropagating the critic’s gradient through the entire diffusion chain (BPTT). While more effective for maximization, BPTT through dozens of denoising steps is computationally prohibitive and prone to vanishing or exploding gradients.

**The Shift to Efficient One-step Flows.** To overcome the stability and efficiency bottlenecks of BPTT, the field has shifted towards *Flow Matching* (Lipman et al., 2023), which admits straighter generation paths. **FQL** (Park et al., 2025c) pioneered this direction by distilling the flow into a **one-step** policy. This allows FQL to bypass BPTT entirely, applying critic gradients directly to the single-step output. Similarly, **MeanFlow-QL** (Wang et al., 2025) and **SORL** (Espinosa-Dice et al., 2025) leverage mean flows or shortcut models to achieve similar one-step efficiency. These methods successfully mitigate the computational cost of iterative solvers while enabling direct policy improvement.

**The Expressivity-Optimization Gap.** Despite their efficiency, one-step approaches face a critical limitation: Expressivity. Collapsing the generation process into a single step can limit the model’s ability to capture the highly multimodal and complex distributions present in large-scale datasets (e.g., OGBench). To address this, **SACFlow** (Zhang et al., 2025b) re-introduces multi-step generation parameterized by GRUs (Cho et al., 2014)/Transformers (Vaswani et al., 2017), but this necessitates bringing back BPTT, re-introducing stability concerns. Crucially, *all* the aforementioned methods (FQL, SACFlow, etc.) suffer from the **Joint Optimization Conflict**: they train a single network to simultaneously minimize BC loss and maximize Q-value. This requires a delicate balancing coefficient; if the Q-loss dominates, the flow manifold collapses (destroying the constraint); if BC dominates, improvement is negligible.

**Contextualizing DeFlow.** DeFlow resolves these conflicts via decoupling. Unlike one-step methods (FQL, MeanFlow-QL) that compromise modeling power for efficiency, we utilize a multi-step flow solely for pure BC, ensuring maximum expressivity and constraint satisfaction. Unlike joint opti-

mization methods (SACFlow, Diffusion-QL) that struggle with BPTT or loss balancing, we perform policy improvement via a separate, lightweight Refinement MLP. This allows DeFlow to combine the high-fidelity modeling of iterative flows with the stable, efficient maximization of standard actor-critic algorithms.

*Note on Value Modeling:* While our focus is on policy extraction, flow matching has also been applied to model value distributions, as seen in **floq** (Agrawalla et al., 2025) and **Value Flows** (Dong et al., 2025). These works are orthogonal to our contribution and can potentially be combined with DeFlow’s policy refinement framework.

## 4.2. Residual Learning

The idea of residual learning has a rich history in machine learning, from ResNets (He et al., 2016) in computer vision to residual policy learning in robotics (Silver et al., 2019). We have discussed the distinction between **Policy-level Residuals** and our **Instance-level Refinement** in detail in the previous section. Most similarly, Ankile et al. (2025); Xiao et al. (2025) also train a refinement module to adjust actions sampled from a frozen policy with online interactions. Our formulation mainly focuses on balancing BC and Q-learning (the *policy extraction problem*) in offline RL.

## 5. Experiments

In this section, we conduct a series of empirical evaluations to assess the efficacy of DeFlow. Our experiments are conducted on 73 challenging offline RL tasks and 15 O2O RL tasks.

### 5.1. Experimental Setup

**Benchmarks.** We adopt the OGBench task suite (Park et al., 2025a) as our primary evaluation platform. Unlike the now-saturated D4RL benchmarks, OGBench provides a more diverse and challenging set of robotic locomotion and manipulation tasks. We utilize the reward-based “single-task” variants, encompassing 50 state-based tasks (across locomotion and manipulation) and 5 high-dimensional visual manipulation tasks ( $64 \times 64$  pixels). To ensure a comprehensive evaluation, we also include 18 classic tasks from D4RL (Fu et al., 2020), which remain challenging due to their sparse rewards and narrow data distributions.

**Baselines.** Following the standard set in FQL (Park et al., 2025c), we compare DeFlow against nine representative baselines across three paradigms: (1) **Gaussian Policies**: IQL (Kostrikov et al., 2022) and ReBRAC (Tarasov et al., 2023a); (2) **Diffusion Policies**: IDQL (Hansen-Estruch et al., 2023), SRPO (Chen et al., 2024), and Consistency

AC (Ding & Jin, 2024); (3) **Flow-based Methods**: To isolate the benefits of our decoupled refinement, we benchmark flow-based counterparts of existing algorithms (FAWAC, FBRAC, IFQL) and FQL itself. Notably, **SORL** (Espinosa-Dice et al., 2025), **MeanFlow**-QL (Wang et al., 2025) and **SACFlow** (Zhang et al., 2025b) are excluded from our primary benchmark due to their distinct requirements, such as sequential scaling and best-of- $N$  sampling at test time, *etc.* These components deviate from the standard policy extraction setting investigated in this work; we refer interested readers to the original studies for their specific performance characteristics.

**Offline-to-online Experiments.** For O2O experiments, we further compare against **Cal-QL** (Nakamoto et al., 2023) and **RLPD** (Ball et al., 2023), which are specifically engineered for online adaptation. We adapt DeFlow for this setting by simply augmenting the offline dataset  $\mathcal{D}$  with an online replay buffer during training.

**Evaluation Protocol.** We strictly follow the OGBench protocol (Park et al., 2025a), reporting performance after a fixed number of gradient steps rather than the maximum over epochs. Results are averaged over 8 seeds for state-based tasks and 4 seeds for pixel-based tasks (mean  $\pm$  std). We **bold** scores that are within 95% of the best performance. Implementation details are provided in the Appendix.

### 5.2. Results and Analysis

We analyze the properties of our method through the following question:

#### Q: Can we set $\delta$ without extensive tuning?

**Yes, by treating it as a semantic constraint rather than an abstract weight.** Unlike the behavioral cloning weight  $\alpha$ , which often requires extensive tuning,  $\delta$  represents a physical constraint reflecting the *action manifold width*. To quantify this, we compute the *Intrinsic Action Variance* (IAV, denoted as  $\bar{\sigma}_{\text{data}}^2$ ) using the average variance of actions among  $k$ -nearest neighbors. Empirically, we set  $\delta$  proportional to the estimated deviation (e.g.,  $\delta \approx 0.1\bar{\sigma}_{\text{data}}$  for fine manipulation and  $\approx \bar{\sigma}_{\text{data}}$  for navigation). Crucially, our adaptive Lagrangian multiplier ensures robustness to rough estimates of  $\delta$ , effectively eliminating the need for grid search.<sup>1</sup>

#### Q: How does DeFlow compare with SOTA offline RL methods?

**A:** Table 1 presents aggregated results across 73 state and pixel-based tasks.

DeFlow achieves SOTA or near-SOTA performance on

<sup>1</sup>For standard D4RL tasks,  $\delta$  can simply be set based on data quality, *e.g.*,  $10^{-3}$  for expert datasets. See Section A.1 for details.

**Table 1. Offline RL results.** DeFlow achieves state-of-the-art or competitive performance across **73** diverse benchmark tasks, significantly outperforming baselines on complex environments such as `cube-double-play` and `puzzle-3x3-play`. We follow the standard evaluation protocol from Park et al. (2025c). Results are averaged over 8 seeds (4 for pixel-based tasks) and the values are taken from prior works (Tarasov et al., 2023b; Hansen-Estruch et al., 2023; Chen et al., 2024; Park et al., 2025c). See Table 6 for the full results.

Task Category	Gaussian Policies			Diffusion Policies			Flow Policies				
	BC	IQL	ReBRAC	IDQL	SRPO	CAC	FAWAC	FBRAC	IFQL	FQL	DeFlow
OGBench antmaze-large-singletask (5 tasks)	11 $\pm$ 1	53 $\pm$ 3	<b>81 <math>\pm</math> 5</b>	21 $\pm$ 5	11 $\pm$ 4	33 $\pm$ 4	6 $\pm$ 1	60 $\pm$ 6	28 $\pm$ 5	<b>79 <math>\pm</math> 3</b>	<b>81 <math>\pm</math> 3</b>
OGBench antmaze-giant-singletask (5 tasks)	0 $\pm$ 0	4 $\pm$ 1	<b>26 <math>\pm</math> 8</b>	0 $\pm$ 0	0 $\pm$ 0	0 $\pm$ 0	0 $\pm$ 0	4 $\pm$ 4	3 $\pm$ 2	9 $\pm$ 6	12 $\pm$ 5
OGBench humanoidmaze-medium-singletask (5 tasks)	2 $\pm$ 1	33 $\pm$ 2	22 $\pm$ 8	1 $\pm$ 0	1 $\pm$ 1	53 $\pm$ 8	19 $\pm$ 1	38 $\pm$ 5	<b>60 <math>\pm</math> 14</b>	<b>58 <math>\pm</math> 5</b>	48 $\pm$ 4
OGBench humanoidmaze-large-singletask (5 tasks)	1 $\pm$ 0	2 $\pm$ 1	2 $\pm$ 1	1 $\pm$ 0	0 $\pm$ 0	0 $\pm$ 0	0 $\pm$ 0	2 $\pm$ 0	<b>11 <math>\pm</math> 2</b>	4 $\pm$ 2	5 $\pm$ 2
OGBench antsoccer-arena-singletask (5 tasks)	1 $\pm$ 0	8 $\pm$ 2	0 $\pm$ 0	12 $\pm$ 4	1 $\pm$ 0	2 $\pm$ 4	12 $\pm$ 0	16 $\pm$ 1	33 $\pm$ 6	60 $\pm$ 2	<b>67 <math>\pm</math> 3</b>
OGBench cube-single-singletask (5 tasks)	5 $\pm$ 1	83 $\pm$ 3	91 $\pm$ 2	<b>95 <math>\pm</math> 2</b>	80 $\pm$ 5	85 $\pm$ 9	81 $\pm$ 4	79 $\pm$ 7	79 $\pm$ 2	<b>96 <math>\pm</math> 1</b>	<b>96 <math>\pm</math> 2</b>
OGBench cube-double-singletask (5 tasks)	2 $\pm$ 1	7 $\pm$ 1	12 $\pm$ 1	15 $\pm$ 6	2 $\pm$ 1	6 $\pm$ 2	5 $\pm$ 2	15 $\pm$ 3	14 $\pm$ 3	29 $\pm$ 2	<b>40 <math>\pm</math> 5</b>
OGBench scene-singletask (5 tasks)	5 $\pm$ 1	28 $\pm$ 1	41 $\pm$ 3	46 $\pm$ 3	20 $\pm$ 1	40 $\pm$ 7	30 $\pm$ 3	45 $\pm$ 5	30 $\pm$ 3	<b>56 <math>\pm</math> 2</b>	51 $\pm$ 3
OGBench puzzle-3x3-singletask (5 tasks)	2 $\pm$ 0	9 $\pm$ 1	21 $\pm$ 1	10 $\pm$ 2	18 $\pm$ 1	19 $\pm$ 0	6 $\pm$ 2	14 $\pm$ 4	19 $\pm$ 1	30 $\pm$ 1	<b>43 <math>\pm</math> 4</b>
OGBench puzzle-4x4-singletask (5 tasks)	0 $\pm$ 0	7 $\pm$ 1	14 $\pm$ 1	<b>29 <math>\pm</math> 3</b>	10 $\pm$ 3	15 $\pm$ 3	1 $\pm$ 0	13 $\pm$ 1	25 $\pm$ 5	17 $\pm$ 2	11 $\pm$ 2
D4RL antmaze (6 tasks)	17	57	78	79	74	30 $\pm$ 3	44 $\pm$ 3	64 $\pm$ 7	65 $\pm$ 7	<b>84 <math>\pm</math> 3</b>	<b>83 <math>\pm</math> 2</b>
D4RL adroit (12 tasks)	48	53	<b>59</b>	52 $\pm$ 1	51 $\pm$ 1	43 $\pm$ 2	48 $\pm$ 1	50 $\pm$ 2	52 $\pm$ 1	52 $\pm$ 1	52 $\pm$ 1
Visual manipulation (5 tasks)	-	42 $\pm$ 4	60 $\pm$ 2	-	-	-	-	22 $\pm$ 2	50 $\pm$ 5	65 $\pm$ 2	<b>69 <math>\pm</math> 2</b>

<sup>1</sup> Due to the high computational cost of pixel-based tasks, we selectively benchmark 5 methods that achieve strong performance on state-based OGBench tasks.

**Table 2. Offline-to-online RL results.** The results are averaged over 8 seeds unless otherwise mentioned.

Task	IQL	ReBRAC	Cal-QL	RLPD	IFQL	FQL	DeFlow
humanoidmaze-medium-navigate-singletask-v0	21 $\pm$ 13 $\rightarrow$ 16 $\pm$ 8	16 $\pm$ 20 $\rightarrow$ 1 $\pm$ 1	0 $\pm$ 0 $\rightarrow$ 0 $\pm$ 0	0 $\pm$ 0 $\rightarrow$ 8 $\pm$ 10	56 $\pm$ 35 $\rightarrow$ <b>82 <math>\pm</math> 20</b>	12 $\pm$ 7 $\rightarrow$ 22 $\pm$ 12	13 $\pm$ 5 $\rightarrow$ 65 $\pm$ 12
antsoccer-arena-navigate-singletask-v0	2 $\pm$ 1 $\rightarrow$ 0 $\pm$ 0	0 $\pm$ 0 $\rightarrow$ 0 $\pm$ 0	0 $\pm$ 0 $\rightarrow$ 0 $\pm$ 0	0 $\pm$ 0 $\rightarrow$ 0 $\pm$ 0	26 $\pm$ 15 $\rightarrow$ 39 $\pm$ 10	28 $\pm$ 8 $\rightarrow$ <b>86 <math>\pm</math> 5</b>	44 $\pm$ 8 $\rightarrow$ <b>86 <math>\pm</math> 3</b>
cube-double-play-singletask-v0	0 $\pm$ 1 $\rightarrow$ 0 $\pm$ 0	6 $\pm$ 5 $\rightarrow$ 28 $\pm$ 8	0 $\pm$ 0 $\rightarrow$ 0 $\pm$ 0	0 $\pm$ 0 $\rightarrow$ 0 $\pm$ 0	12 $\pm$ 9 $\rightarrow$ 40 $\pm$ 5	40 $\pm$ 11 $\rightarrow$ <b>92 <math>\pm</math> 3</b>	48 $\pm$ 13 $\rightarrow$ <b>93 <math>\pm</math> 4</b>
scene-play-singletask-v0	14 $\pm$ 11 $\rightarrow$ 10 $\pm$ 9	55 $\pm$ 10 $\rightarrow$ <b>100 <math>\pm</math> 0</b>	1 $\pm$ 2 $\rightarrow$ 50 $\pm$ 53	0 $\pm$ 0 $\rightarrow$ 100 $\pm$ 0	0 $\pm$ 1 $\rightarrow$ 60 $\pm$ 39	82 $\pm$ 11 $\rightarrow$ <b>100 <math>\pm</math> 1</b>	58 $\pm$ 14 $\rightarrow$ <b>100 <math>\pm</math> 1</b>
puzzle-4x4-play-singletask-v0	5 $\pm$ 2 $\rightarrow$ 1 $\pm$ 1	8 $\pm$ 4 $\rightarrow$ 14 $\pm$ 5	0 $\pm$ 0 $\rightarrow$ 0 $\pm$ 0	0 $\pm$ 0 $\rightarrow$ <b>100 <math>\pm</math> 1</b>	23 $\pm$ 6 $\rightarrow$ 19 $\pm$ 33	8 $\pm$ 3 $\rightarrow$ 38 $\pm$ 52	<b>4 <math>\pm</math> 1 <math>\rightarrow</math> 100 <math>\pm</math> 0</b>
antmaze-umaze-v2	77 $\rightarrow$ <b>96</b>	98 $\rightarrow$ 75	77 $\rightarrow$ <b>100</b>	0 $\pm$ 0 $\rightarrow$ <b>98 <math>\pm</math> 3</b>	94 $\pm$ 5 $\rightarrow$ <b>96 <math>\pm</math> 2</b>	97 $\pm$ 2 $\rightarrow$ 99 $\pm$ 1	96 $\pm$ 3 $\rightarrow$ <b>99 <math>\pm</math> 2</b>
antmaze-umaze-diverse-v2	60 $\rightarrow$ 64	74 $\rightarrow$ <b>98</b>	32 $\rightarrow$ <b>98</b>	0 $\pm$ 0 $\rightarrow$ 94 $\pm$ 5	69 $\pm$ 20 $\rightarrow$ 93 $\pm$ 5	79 $\pm$ 16 $\rightarrow$ <b>100 <math>\pm</math> 1</b>	87 $\pm$ 6 $\rightarrow$ <b>99 <math>\pm</math> 1</b>
antmaze-medium-play-v2	72 $\rightarrow$ 90	88 $\rightarrow$ <b>98</b>	72 $\rightarrow$ <b>99</b>	0 $\pm$ 0 $\rightarrow$ <b>98 <math>\pm</math> 2</b>	52 $\pm$ 19 $\rightarrow$ 93 $\pm$ 2	77 $\pm$ 7 $\rightarrow$ <b>97 <math>\pm</math> 2</b>	76 $\pm$ 5 $\rightarrow$ <b>97 <math>\pm</math> 2</b>
antmaze-medium-diverse-v2	64 $\rightarrow$ 92	85 $\rightarrow$ <b>99</b>	62 $\rightarrow$ <b>98</b>	0 $\pm$ 0 $\rightarrow$ <b>97 <math>\pm</math> 2</b>	44 $\pm$ 26 $\rightarrow$ 89 $\pm$ 4	55 $\pm$ 19 $\rightarrow$ <b>97 <math>\pm</math> 3</b>	61 $\pm$ 9 $\rightarrow$ <b>98 <math>\pm</math> 2</b>
antmaze-large-play-v2	38 $\rightarrow$ 64	68 $\rightarrow$ 32	32 $\rightarrow$ <b>97</b>	0 $\pm$ 0 $\rightarrow$ <b>93 <math>\pm</math> 5</b>	64 $\pm$ 14 $\rightarrow$ 80 $\pm$ 5	66 $\pm$ 40 $\rightarrow$ 84 $\pm$ 30	76 $\pm$ 6 $\rightarrow$ <b>95 <math>\pm</math> 4</b>
antmaze-large-diverse-v2	27 $\rightarrow$ 64	67 $\rightarrow$ 72	44 $\rightarrow$ <b>92</b>	0 $\pm$ 0 $\rightarrow$ <b>94 <math>\pm</math> 3</b>	69 $\pm$ 6 $\rightarrow$ 86 $\pm$ 5	75 $\pm$ 24 $\rightarrow$ <b>94 <math>\pm</math> 3</b>	76 $\pm$ 9 $\rightarrow$ <b>96 <math>\pm</math> 2</b>
pen-cloned-v1	84 $\rightarrow$ 102	74 $\rightarrow$ 138	-3 $\rightarrow$ -3	3 $\pm$ 2 $\rightarrow$ 120 $\pm$ 10	77 $\pm$ 7 $\rightarrow$ 107 $\pm$ 10	53 $\pm$ 14 $\rightarrow$ <b>149 <math>\pm</math> 6</b>	64 $\pm$ 13 $\rightarrow$ <b>142 <math>\pm</math> 7</b>
door-cloned-v1	1 $\rightarrow$ 20	0 $\rightarrow$ <b>102</b>	-0 $\rightarrow$ -0	0 $\pm$ 0 $\rightarrow$ <b>102 <math>\pm</math> 7</b>	3 $\pm$ 2 $\rightarrow$ 50 $\pm$ 15	0 $\pm$ 0 $\rightarrow$ <b>102 <math>\pm</math> 5</b>	0 $\pm$ 0 $\rightarrow$ <b>99 <math>\pm</math> 2</b>
hammer-cloned-v1	1 $\rightarrow$ 57	7 $\rightarrow$ <b>125</b>	0 $\rightarrow$ 0	0 $\pm$ 0 $\rightarrow$ <b>128 <math>\pm</math> 29</b>	4 $\pm$ 2 $\rightarrow$ 60 $\pm$ 14	0 $\pm$ 0 $\rightarrow$ <b>127 <math>\pm</math> 17</b>	7 $\pm$ 3 $\rightarrow$ 106 $\pm$ 10
relocate-cloned-v1	0 $\rightarrow$ 0	1 $\rightarrow$ 7	-0 $\rightarrow$ -0	0 $\pm$ 0 $\rightarrow$ 2 $\pm$ 2	-0 $\pm$ 0 $\rightarrow$ 5 $\pm$ 3	0 $\pm$ 1 $\rightarrow$ <b>62 <math>\pm</math> 8</b>	<b>1 <math>\pm</math> 0 <math>\rightarrow</math> 35 <math>\pm</math> 8</b>

the majority of benchmarks, with significant margins in highly multimodal tasks like `cube-double-play` and `puzzle-3x3-play`. This superiority validates DeFlow’s capability to model complex action distributions where prior methods struggle due to limited expressivity. Notably, DeFlow achieves these results **without extensive hyperparameter tuning**, demonstrating both robustness and simplicity.

### Q: Why does DeFlow outperform one-step baselines in complex tasks?

**A:** To answer this, we visualize the action landscapes of critical states in `cube-double-play` (Figure 2). We identify two primary failure modes in one-step methods like FQL: (i) **Mode Collapse**, where the policy prematurely averages distinct modes into a single, often invalid, mean action (Figure 2a); (ii) **OOD Drift**, where aggressive value maximization drives actions off the data manifold (Figure 2b). In contrast, DeFlow mitigates these issues through its decoupled architecture. The multi-step Base Flow robustly captures the multimodal topology of the data, acting as an anchor. The Refinement Module then performs constrained, local adjustments. This design ensures that policy improvements remain strictly within the valid support, which is decisive

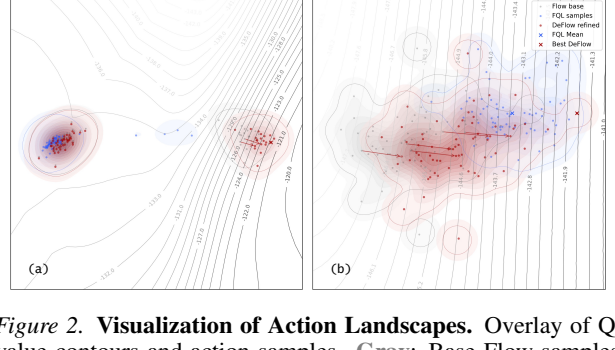


**Figure 2. Visualization of Action Landscapes.** Overlay of Q-value contours and action samples. Gray: Base Flow samples (data proxy); Blue: FQL (one-step); Red: DeFlow (ours). Arrows indicate the refinement trajectory. By anchoring optimization to the Base Flow manifold, DeFlow avoids (a) mode collapse and (b) OOD drift, effectively refining actions within the valid support.

for high-precision manipulation tasks.

### Q: How does DeFlow facilitate stable and efficient O2O training?

**A:** Table 2 and Figure 3 summarize the results across 15 tasks. Quantitatively, DeFlow matches or exceeds the state-

of-the-art (e.g., FQL), achieving remarkable gains in complex tasks like humanoidmaze-medium. A critical advantage of DeFlow is its **seamless transition** from offline to online. Unlike prior works (Park et al., 2025c; Agrawalla et al., 2025) that often necessitate altering hyperparameters (or “loosening” constraints) to encourage exploration, DeFlow requires **zero additional tuning**. We maintain the exact offline configuration, relying on our automatic  $\alpha$  tuning to naturally balance exploration. While this strict adherence to a unified protocol may limit performance in tasks with poor data quality (e.g., relocate-cloned), it ensures empirical rigor and demonstrates the method’s inherent robustness without task-specific engineering.

#### Q: Can we fix the behavior prior in online finetuning?

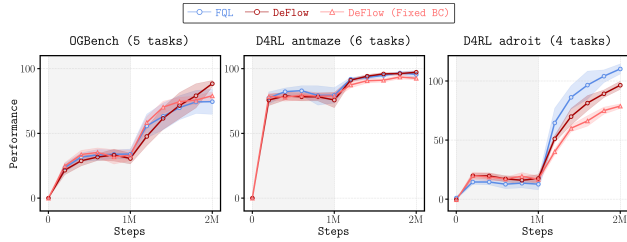


Figure 3. Offline-to-online RL results (8 seeds).

**A: Yes.** Our decoupled design offers a unique efficiency benefit: we can freeze the generative behavior prior (Base Flow) and solely rely on the adaptive  $\alpha$  to modulate exploration. As shown in Figure 3, freezing the prior yields performance competitive with full fine-tuning. This strategy reduces computational overhead (runtime analysis provided in Section B) and enhances stability by eliminating the moving target problem. Crucially, it provides a scalable pathway for finetuning large-scale foundation models, where updating the generative backbone online is computationally prohibitive.

#### Q: Can we combine DeFlow with value modeling methods?

Table 3. Success rates on manipulation tasks when combining DeFlow with floq’s value function.

Task	FQL	floq	DeFlow	DeFlow+floq
cube-double-play	$25 \pm 6$	$47 \pm 15$	$40 \pm 5$	<b><math>58 \pm 5</math></b>
puzzle-3x3-play	$29 \pm 5$	$37 \pm 7$	$43 \pm 4$	<b><math>50 \pm 3</math></b>

**A: Yes.** While our focus is on policy extraction, DeFlow’s refinement framework is orthogonal to value modeling techniques like floq (Agrawalla et al., 2025). As shown in Table 3, we directly integrate DeFlow with floq’s value function and observe synergistic improvements without any tuning, suggesting that DeFlow can serve as a versatile policy extraction module compatible with advanced value estimators.

## 6. Discussions and Conclusion

In this paper, we present DeFlow, a framework for offline RL that decouples high-fidelity behavior modeling from value-driven policy refinement. By leveraging multi-step flow matching for behavior cloning and a lightweight refinement module for Q-value maximization, DeFlow effectively resolves the expressivity-optimization conflict inherent in prior methods. Our extensive empirical evaluations across 73 offline RL tasks and 15 O2O tasks demonstrate that DeFlow achieves comparable performance against SOTA with minimal hyperparameter tuning, highlighting its robustness and practicality. As a closing remark, rather than claiming DeFlow as a definitive solution, we position it as a lens to re-examine the interplay between generative diversity and critic-guided optimization. Our findings suggest that while modeling the behavior distribution is a solved problem with modern generative models, effective policy extraction remains a nuanced challenge where “more optimization” does not always equate to better performance.

**The Saturation of Inference Scaling.** A pivotal insight from our analysis is the counter-intuitive behavior of inference-time scaling. We observed that standard strategies like rejection sampling yield minimal gains within our framework. We attribute this to a **Trust Region Saturation** phenomenon: DeFlow’s refinement module is designed to be aggressive—it efficiently pushes the proposal to the boundary of the manifold constraint ( $\|\Delta a\|^2 \approx \delta$ ) in a single forward pass. Consequently, the “optimization budget” allowed by the behavior prior is fully consumed. Any further attempts to maximize Q-values (e.g., via rejection sampling) tend to exploit the critic’s approximation errors (adversarial OOD peaks) rather than uncovering legitimate high-value modes. This reveals a critical boundary in offline RL: simply “sampling more” is futile when the valid optimization landscape is already saturated.

**Rethinking Policy Extraction.** This finding suggests that the bottleneck in modern offline RL has shifted. The challenge is no longer about *generating* diverse behaviors (which flow models handle well), but about *navigating* the treacherous signal-to-noise ratio of the learned Q-function. DeFlow demonstrates that a deterministic, constrained gradient step could be safer and more effective than stochastic search in this landscape. Looking forward, we posit that the next breakthrough lies not in blind maximization, but in **Manifold-Aware Sampling**—incorporating methods like constrained Langevin dynamics or gradient-guided flow that can explore the value landscape while explicitly adhering to the complex topology of the behavior manifold, thereby avoiding the OOD pitfalls that plague current extraction techniques.

## Impact Statement

This paper presents work whose goal is to advance the field of Machine Learning. There are many potential societal consequences of our work, none which we feel must be specifically highlighted here.

## References

Agrawalla, B., Nauman, M., Agrawal, K., and Kumar, A. floq: Training critics via flow-matching for scaling compute in value-based rl. *arXiv preprint arXiv:2509.06863*, 2025.

Ankile, L., Simeonov, A., Shenfeld, I., Torne, M., and Agrawal, P. From imitation to refinement – residual rl for precise assembly. In *2025 IEEE International Conference on Robotics and Automation (ICRA)*, pp. 01–08. IEEE, 2025.

Ball, P. J., Smith, L., Kostrikov, I., and Levine, S. Efficient online reinforcement learning with offline data. In *International Conference on Machine Learning (ICML)*, 2023.

Chen, H., Lu, C., Wang, Z., Su, H., and Zhu, J. Score regularized policy optimization through diffusion behavior. In *International Conference on Learning Representations (ICLR)*, 2024.

Cho, K., van Merriënboer, B., Çaglar Gülcöhre, Bahdanau, D., Bougares, F., Schwenk, H., and Bengio, Y. Learning phrase representations using rnn encoder–decoder for statistical machine translation. In *Conference on Empirical Methods in Natural Language Processing (EMNLP)*, 2014.

Ding, Z. and Jin, C. Consistency models as a rich and efficient policy class for reinforcement learning. In *International Conference on Learning Representations (ICLR)*, 2024.

Dong, P., Zheng, C., Finn, C., Sadigh, D., and Eysenbach, B. Value flows, 2025. URL <https://arxiv.org/abs/2510.07650>.

Espinosa-Dice, N., Zhang, Y., Chen, Y., Guo, B., Oertell, O., Swamy, G., Brantley, K., and Sun, W. Scaling offline rl via efficient and expressive shortcut models. *arXiv preprint arXiv:2505.22866*, 2025.

Fu, J., Kumar, A., Nachum, O., Tucker, G., and Levine, S. D4rl: Datasets for deep data-driven reinforcement learning. *ArXiv*, abs/2004.07219, 2020.

Fujimoto, S. and Gu, S. S. A minimalist approach to offline reinforcement learning. In *Neural Information Processing Systems (NeurIPS)*, 2021.

Haarnoja, T., Zhou, A., Abbeel, P., and Levine, S. Soft actor-critic: Off-policy maximum entropy deep reinforcement learning with a stochastic actor. In *arXiv*, 2018. URL <https://arxiv.org/pdf/1801.01290.pdf>.

Hansen-Estruch, P., Kostrikov, I., Janner, M., Kuba, J. G., and Levine, S. Idql: Implicit q-learning as an actor-critic method with diffusion policies. *ArXiv*, abs/2304.10573, 2023.

He, K., Zhang, X., Ren, S., and Sun, J. Deep residual learning for image recognition. In *Proceedings of the IEEE conference on computer vision and pattern recognition*, pp. 770–778, 2016.

Janner, M., Du, Y., Tenenbaum, J. B., and Levine, S. Planning with diffusion for flexible behavior synthesis. In *International Conference on Machine Learning (ICML)*, 2022.

Kang, B., Ma, X., Du, C., Pang, T., and Yan, S. Efficient diffusion policies for offline reinforcement learning. In *Neural Information Processing Systems (NeurIPS)*, 2023.

Kostrikov, I., Nair, A., and Levine, S. Offline reinforcement learning with implicit q-learning. In *International Conference on Learning Representations (ICLR)*, 2022.

Kumar, A., Zhou, A., Tucker, G., and Levine, S. Conservative q-learning for offline reinforcement learning. In *Neural Information Processing Systems (NeurIPS)*, 2020.

Levine, S., Kumar, A., Tucker, G., and Fu, J. Offline reinforcement learning: Tutorial, review, and perspectives on open problems. *arXiv preprint*, 2020.

Lillicrap, T. P., Hunt, J. J., Pritzel, A., Heess, N. M. O., Erez, T., Tassa, Y., Silver, D., and Wierstra, D. Continuous control with deep reinforcement learning. In *International Conference on Learning Representations (ICLR)*, 2016.

Lipman, Y., Chen, R. T., Ben-Hamu, H., Nickel, M., and Le, M. Flow matching for generative modeling. In *International Conference on Learning Representations (ICLR)*, 2023.

Lipman, Y., Havasi, M., Holderrieth, P., Shaul, N., Le, M., Karrer, B., Chen, R. T. Q., Lopez-Paz, D., Ben-Hamu, H., and Gat, I. Flow matching guide and code. *ArXiv*, abs/2412.06264, 2024.

Lu, C., Ball, P., Teh, Y. W., and Parker-Holder, J. Synthetic experience replay. In *Neural Information Processing Systems (NeurIPS)*, 2023a.

Lu, C., Chen, H., Chen, J., Su, H., Li, C., and Zhu, J. Contrastive energy prediction for exact energy-guided diffusion sampling in offline reinforcement learning. In

*International Conference on Machine Learning (ICML)*, 2023b.

Mnih, V., Kavukcuoglu, K., Silver, D., Graves, A., Antonoglou, I., Wierstra, D., and Riedmiller, M. A. Playing atari with deep reinforcement learning. *ArXiv*, abs/1312.5602, 2013.

Nakamoto, M., Zhai, Y., Singh, A., Mark, M. S., Ma, Y., Finn, C., Kumar, A., and Levine, S. Cal-ql: Calibrated offline rl pre-training for efficient online fine-tuning. In *Neural Information Processing Systems (NeurIPS)*, 2023.

Park, S., Frans, K., Eysenbach, B., and Levine, S. Ogbench: Benchmarking offline goal-conditioned rl. In *International Conference on Learning Representations (ICLR)*, 2025a.

Park, S., Frans, K., Mann, D., Eysenbach, B., Kumar, A., and Levine, S. Horizon reduction makes rl scalable, 2025b. URL <https://arxiv.org/abs/2506.04168>.

Park, S., Li, Q., and Levine, S. Flow q-learning. *ArXiv*, abs/2502.02538, 2025c.

Park, S., Mann, D., and Levine, S. Dual goal representations, 2025d. URL <https://arxiv.org/abs/2510.06714>.

Park, S., Oberai, A., Atreya, P., and Levine, S. Transitive rl: Value learning via divide and conquer, 2025e. URL <https://arxiv.org/abs/2510.22512>.

Peng, X. B., Kumar, A., Zhang, G., and Levine, S. Advantage-weighted regression: Simple and scalable off-policy reinforcement learning. *ArXiv*, abs/1910.00177, 2019.

Puterman, M. L. *Markov decision processes: discrete stochastic dynamic programming*. John Wiley & Sons, 2014.

Silver, T., Allen, K., Tenenbaum, J., and Kaelbling, L. Residual policy learning, 2019. URL <https://arxiv.org/abs/1812.06298>.

Sohl-Dickstein, J., Weiss, E., Maheswaranathan, N., and Ganguli, S. Deep unsupervised learning using nonequilibrium thermodynamics. In *International Conference on Machine Learning (ICML)*, 2015.

Tarasov, D., Kurenkov, V., Nikulin, A., and Kolesnikov, S. Revisiting the minimalist approach to offline reinforcement learning. In *Neural Information Processing Systems (NeurIPS)*, 2023a.

Tarasov, D., Nikulin, A., Akimov, D., Kurenkov, V., and Kolesnikov, S. Corl: Research-oriented deep offline reinforcement learning library. In *Neural Information Processing Systems (NeurIPS)*, 2023b.

Vaswani, A., Shazeer, N., Parmar, N., Uszkoreit, J., Jones, L., Gomez, A. N., Kaiser, Ł., and Polosukhin, I. Attention is all you need. *Advances in neural information processing systems*, 30, 2017.

Wang, Z., Hunt, J. J., and Zhou, M. Diffusion policies as an expressive policy class for offline reinforcement learning. In *International Conference on Learning Representations (ICLR)*, 2023.

Wang, Z., Li, D., Chen, Y., Shi, Y., Bai, L., Yu, T., and Fu, Y. One-step generative policies with q-learning: A reformulation of meanflow. *arXiv preprint arXiv:2511.13035*, 2025.

Xiao, W., Lin, H., Peng, A., Xue, H., He, T., Xie, Y., Hu, F., Wu, J., Luo, Z., Fan, L. J., Shi, G., and Zhu, Y. Self-improving vision-language-action models with data generation via residual rl, 2025. URL <https://arxiv.org/abs/2511.00091>.

Xu, H., Jiang, L., Li, J., Yang, Z., Wang, Z., Chan, V., and Zhan, X. Offline rl with no ood actions: In-sample learning via implicit value regularization. In *International Conference on Learning Representations (ICLR)*, 2023.

Zhang, S., Zhang, W., and Gu, Q. Energy-weighted flow matching for offline reinforcement learning. In *International Conference on Learning Representations (ICLR)*, 2025a.

Zhang, Y., Yu, S., Zhang, T., Guang, M., Hui, H., Long, K., Wang, Y., Yu, C., and Ding, W. Sac flow: Sample-efficient reinforcement learning of flow-based policies via velocity-reparameterized sequential modeling, 2025b. URL <https://arxiv.org/abs/2509.25756>.

## A. Implementation Details

We implement DeFlow based on the FQL (Park et al., 2025c) and floq (Agrawalla et al., 2025) codebases. The flow model architecture follows the same design as FQL, using a 4-layer MLP with 512 hidden units. The refinement module uses the same architecture for clear comparison. We use Q-Normalization as in FQL to stabilize Q-value scales across different tasks. For other hyperparameters except the target divergence  $\delta$ , we follow the FQL/floq’s default settings.

### A.1. Hyperparameter Settings

For the target divergence  $\delta$ , we set it based on the estimated Intrinsic Action Variance (IAV) of the dataset. Specifically, we compute the average variance of actions among  $k$ -nearest neighbors ( $k = 5$ ) for each state in the following tasks and normalize it by the action dimension:

	cube-double	antmaze-large	puzzle-3x3	antsoccer
IAV	0.013	0.018	0.007	0.026

Leveraging prior knowledge of task complexity (Park et al., 2025a), we observe a strong empirical correlation between the Intrinsic Action Variance (IAV) and the optimal constraint  $\delta$ :

- **Fine Manipulation** (e.g., cube-double-play): High precision requires a tighter constraint,  $\delta \approx 0.1 \times \text{IAV}$ .
- **Navigation/Locomotion** (e.g., antsoccer): Higher tolerance allows a looser constraint,  $\delta \approx 1.0 \times \text{IAV}$ .
- **D4RL Benchmarks**: A generic setting suffices based on data quality (e.g.,  $\delta = 10^{-3}$ ).

This heuristic contrasts sharply with the exhaustive grid search required for the behavioral cloning weight  $\alpha$  in prior works (Park et al., 2025c). Our method relies only on rough estimates of  $\delta$  inferred from task semantics, drastically reducing tuning effort. Crucially, we maintain the same  $\delta$  for online fine-tuning without further adjustment. While this strict protocol may limit asymptotic performance on specific outlier tasks, it underscores the method’s inherent robustness and eliminates the need for task-specific engineering during the offline-to-online transition. Detailed hyperparameter settings for all experiments are provided in Table 5.

## B. Additional Experimental Results

We report the full offline RL results across all 73 tasks in Table 6. The results are averaged over 8 seeds (4 seeds for pixel-based tasks) and we bold scores that are within 95% of the best performance as in FQL (Park et al., 2025c).

Table 4 compares the training and inference speeds of FQL and DeFlow. The run times are measured on the same machine with an NVIDIA 3090 GPU. Because DeFlow requires the multi-step flow to take samples for Q updates during training, its training time is slightly longer than FQL (while their actor update times are the same). During inference, when the multi-step flow is fixed and only the refinement module is used, DeFlow’s inference time can be faster, which will be more significant when scaling up the flow model.

Table 4. Training and Inference Time Comparison (in milliseconds per step).

Methods	Offline training	Online training	Inference
FQL	$2.2 \pm 1$	$5.1 \pm 0.5$	$4.2 \pm 0.7$
DeFlow	$2.4 \pm 1$	$5.3 \pm 0.4$	$4.5 \pm 0.5$
DeFlow (frozen prior)	-	$5.2 \pm 0.5$	-

Table 5. Task-specific hyperparameters for offline RL. We take hyperparameters from FQL (Park et al., 2025c) for comparison.

Task	IQL $\alpha$	ReBRAC ( $\alpha_1, \alpha_2$ )	IDQL $N$	SRPO $\beta$	CAC $\eta$	FAWAC $\alpha$	FBRAC $\alpha$	IFQL $N$	FQL $\alpha$	DeFlow $\delta$
antmaze-large-navigate-singletask-task1-v0	10	(0.003, 0.01)	32	0.3	1	3	3	32	10	0.01
antmaze-large-navigate-singletask-task2-v0	10	(0.003, 0.01)	32	0.3	1	3	3	32	10	0.01
antmaze-large-navigate-singletask-task3-v0	10	(0.003, 0.01)	32	0.3	1	3	3	32	10	0.01
antmaze-large-navigate-singletask-task4-v0	10	(0.003, 0.01)	32	0.3	1	3	3	32	10	0.01
antmaze-large-navigate-singletask-task5-v0	10	(0.003, 0.01)	32	0.3	1	3	3	32	10	0.01
antmaze-giant-navigate-singletask-task1-v0	10	(0.003, 0.01)	32	0.3	1	3	10	32	10	0.01
antmaze-giant-navigate-singletask-task2-v0	10	(0.003, 0.01)	32	0.3	1	3	10	32	10	0.01
antmaze-giant-navigate-singletask-task3-v0	10	(0.003, 0.01)	32	0.3	1	3	10	32	10	0.01
antmaze-giant-navigate-singletask-task4-v0	10	(0.003, 0.01)	32	0.3	1	3	10	32	10	0.01
antmaze-giant-navigate-singletask-task5-v0	10	(0.003, 0.01)	32	0.3	1	3	10	32	10	0.01
humanoidmaze-medium-navigate-singletask-task1-v0	10	(0.01, 0.01)	32	0.3	0.03	3	30	32	30	0.001
humanoidmaze-medium-navigate-singletask-task2-v0	10	(0.01, 0.01)	32	0.3	0.03	3	30	32	30	0.001
humanoidmaze-medium-navigate-singletask-task3-v0	10	(0.01, 0.01)	32	0.3	0.03	3	30	32	30	0.001
humanoidmaze-medium-navigate-singletask-task4-v0	10	(0.01, 0.01)	32	0.3	0.03	3	30	32	30	0.001
humanoidmaze-medium-navigate-singletask-task5-v0	10	(0.01, 0.01)	32	0.3	0.03	3	30	32	30	0.001
humanoidmaze-large-navigate-singletask-task1-v0	10	(0.01, 0.01)	32	0.3	1	3	30	32	30	0.001
humanoidmaze-large-navigate-singletask-task2-v0	10	(0.01, 0.01)	32	0.3	1	3	30	32	30	0.001
humanoidmaze-large-navigate-singletask-task3-v0	10	(0.01, 0.01)	32	0.3	1	3	30	32	30	0.001
humanoidmaze-large-navigate-singletask-task4-v0	10	(0.01, 0.01)	32	0.3	1	3	30	32	30	0.001
humanoidmaze-large-navigate-singletask-task5-v0	10	(0.01, 0.01)	32	0.3	1	3	30	32	30	0.001
antsoccer-arena-navigate-singletask-task1-v0	1	(0.01, 0.01)	32	0.03	1	10	30	64	10	0.01
antsoccer-arena-navigate-singletask-task2-v0	1	(0.01, 0.01)	32	0.03	1	10	30	64	10	0.01
antsoccer-arena-navigate-singletask-task3-v0	1	(0.01, 0.01)	32	0.03	1	10	30	64	10	0.01
antsoccer-arena-navigate-singletask-task4-v0	1	(0.01, 0.01)	32	0.03	1	10	30	64	10	0.01
antsoccer-arena-navigate-singletask-task5-v0	1	(0.01, 0.01)	32	0.03	1	10	30	64	10	0.01
cube-single-play-singletask-task1-v0	1	(1, 0)	32	0.03	0.003	1	100	32	300	0.001
cube-single-play-singletask-task2-v0	1	(1, 0)	32	0.03	0.003	1	100	32	300	0.001
cube-single-play-singletask-task3-v0	1	(1, 0)	32	0.03	0.003	1	100	32	300	0.001
cube-single-play-singletask-task4-v0	1	(1, 0)	32	0.03	0.003	1	100	32	300	0.001
cube-single-play-singletask-task5-v0	1	(1, 0)	32	0.03	0.003	1	100	32	300	0.001
cube-double-play-singletask-task1-v0	0.3	(0.1, 0)	32	0.1	0.3	0.3	100	32	300	0.001
cube-double-play-singletask-task2-v0	0.3	(0.1, 0)	32	0.1	0.3	0.3	100	32	300	0.001
cube-double-play-singletask-task3-v0	0.3	(0.1, 0)	32	0.1	0.3	0.3	100	32	300	0.001
cube-double-play-singletask-task4-v0	0.3	(0.1, 0)	32	0.1	0.3	0.3	100	32	300	0.001
cube-double-play-singletask-task5-v0	0.3	(0.1, 0)	32	0.1	0.3	0.3	100	32	300	0.001
scene-play-singletask-task1-v0	10	(0.1, 0.01)	32	0.1	0.3	0.3	100	32	300	0.001
scene-play-singletask-task2-v0	10	(0.1, 0.01)	32	0.1	0.3	0.3	100	32	300	0.001
scene-play-singletask-task3-v0	10	(0.1, 0.01)	32	0.1	0.3	0.3	100	32	300	0.001
scene-play-singletask-task4-v0	10	(0.1, 0.01)	32	0.1	0.3	0.3	100	32	300	0.001
scene-play-singletask-task5-v0	10	(0.1, 0.01)	32	0.1	0.3	0.3	100	32	300	0.001
puzzle-3x3-play-singletask-task1-v0	10	(0.3, 0.01)	32	0.1	0.01	0.3	100	32	1000	0.0005
puzzle-3x3-play-singletask-task2-v0	10	(0.3, 0.01)	32	0.1	0.01	0.3	100	32	1000	0.0005
puzzle-3x3-play-singletask-task3-v0	10	(0.3, 0.01)	32	0.1	0.01	0.3	100	32	1000	0.0005
puzzle-3x3-play-singletask-task4-v0	10	(0.3, 0.01)	32	0.1	0.01	0.3	100	32	1000	0.0005
puzzle-3x3-play-singletask-task5-v0	10	(0.3, 0.01)	32	0.1	0.01	0.3	100	32	1000	0.0005
puzzle-4x4-play-singletask-task1-v0	3	(0.3, 0.01)	32	0.1	0.01	0.3	300	32	1000	0.0005
puzzle-4x4-play-singletask-task2-v0	3	(0.3, 0.01)	32	0.1	0.01	0.3	300	32	1000	0.0005
puzzle-4x4-play-singletask-task3-v0	3	(0.3, 0.01)	32	0.1	0.01	0.3	300	32	1000	0.0005
puzzle-4x4-play-singletask-task4-v0	3	(0.3, 0.01)	32	0.1	0.01	0.3	300	32	1000	0.0005
puzzle-4x4-play-singletask-task5-v0	3	(0.3, 0.01)	32	0.1	0.01	0.3	300	32	1000	0.0005
antmaze-umaze-v2	-	-	-	-	0.01	3	10	32	10	0.015
antmaze-umaze-diverse-v2	-	-	-	-	0.01	3	10	32	10	0.015
antmaze-medium-play-v2	-	-	-	-	0.01	3	10	32	10	0.015
antmaze-medium-diverse-v2	-	-	-	-	0.01	3	10	32	10	0.015
antmaze-large-play-v2	-	-	-	-	4.5	3	1	32	3	0.015
antmaze-large-diverse-v2	-	-	-	-	3.5	3	1	32	3	0.015
pen-human-v1	-	-	32	0.03	0.003	0.03	30000	32	10000	0.01
pen-cloned-v1	-	-	32	0.1	0.003	0.3	10000	32	10000	0.01
pen-expert-v1	-	-	32	0.1	0.03	0.1	30000	32	3000	0.01
door-human-v1	-	-	32	0.01	0.03	1	30000	32	30000	0.001
door-cloned-v1	-	-	32	0.03	0.003	1	10000	128	30000	0.001
door-expert-v1	-	-	32	0.01	0.03	3	30000	32	30000	0.001
hammer-human-v1	-	-	128	0.1	0.03	3	30000	32	30000	0.001
hammer-cloned-v1	-	-	32	0.1	0.003	0.03	10000	32	10000	0.001
hammer-expert-v1	-	-	32	0.03	0.03	3	30000	32	30000	0.001
relocate-human-v1	-	-	32	0.03	0.01	0.3	30000	128	10000	0.001
relocate-cloned-v1	-	-	64	0.03	0.01	0.1	3000	32	30000	0.001
relocate-expert-v1	-	-	32	0.01	0.003	1	30000	32	30000	0.001
visual-cube-single-play-singletask-task1-v0	1	(1, 0)	-	-	-	-	100	32	300	0.001
visual-cube-double-play-singletask-task1-v0	0.3	(0.1, 0)	-	-	-	-	100	32	100	0.001
visual-scene-play-singletask-task1-v0	10	(0.1, 0.01)	-	-	-	-	100	32	100	0.001
visual-puzzle-3x3-play-singletask-task1-v0	10	(0.3, 0.01)	-	-	-	-	100	32	300	0.0005
visual-puzzle-4x4-play-singletask-task1-v0	3	(0.3, 0.01)	-	-	-	-	300	32	300	0.0005

**Table 6. Full offline RL results.** We present the full results on the 73 OGBench and D4RL tasks. (\*) indicates the default task in each environment. The results are averaged over 8 seeds (4 seeds for pixel-based tasks) unless otherwise mentioned.

Task	Gaussian Policies			Diffusion Policies			Flow Policies				
	BC	IQL	ReBRAC	IDQL	SRPO	CAC	FAWAC	FBRAC	IFQL	FQL	Deflow
antmaze-large-navigate-singletask-task1-v0 (*)	0 $\pm$ 0	48 $\pm$ 9	91 $\pm$ 10	0 $\pm$ 0	0 $\pm$ 0	42 $\pm$ 7	1 $\pm$ 1	70 $\pm$ 20	24 $\pm$ 17	80 $\pm$ 8	88 $\pm$ 6
antmaze-large-navigate-singletask-task2-v0	6 $\pm$ 3	42 $\pm$ 6	88 $\pm$ 4	14 $\pm$ 8	4 $\pm$ 4	1 $\pm$ 1	0 $\pm$ 1	35 $\pm$ 12	8 $\pm$ 3	57 $\pm$ 10	71 $\pm$ 10
antmaze-large-navigate-singletask-task3-v0	29 $\pm$ 5	72 $\pm$ 7	51 $\pm$ 18	26 $\pm$ 8	3 $\pm$ 2	49 $\pm$ 10	12 $\pm$ 4	83 $\pm$ 15	52 $\pm$ 17	93 $\pm$ 3	88 $\pm$ 5
antmaze-large-navigate-singletask-task4-v0	8 $\pm$ 3	51 $\pm$ 9	84 $\pm$ 7	62 $\pm$ 25	45 $\pm$ 19	17 $\pm$ 6	10 $\pm$ 3	37 $\pm$ 18	18 $\pm$ 8	80 $\pm$ 4	77 $\pm$ 5
antmaze-large-navigate-singletask-task5-v0	10 $\pm$ 3	54 $\pm$ 22	90 $\pm$ 2	2 $\pm$ 2	1 $\pm$ 1	55 $\pm$ 6	9 $\pm$ 5	76 $\pm$ 8	38 $\pm$ 18	83 $\pm$ 4	84 $\pm$ 3
antmaze-giant-navigate-singletask-task1-v0 (*)	0 $\pm$ 0	0 $\pm$ 0	27 $\pm$ 22	0 $\pm$ 0	0 $\pm$ 0	0 $\pm$ 0	0 $\pm$ 1	0 $\pm$ 0	4 $\pm$ 5	4 $\pm$ 4	
antmaze-giant-navigate-singletask-task2-v0	0 $\pm$ 0	1 $\pm$ 1	16 $\pm$ 17	0 $\pm$ 0	0 $\pm$ 0	0 $\pm$ 0	4 $\pm$ 7	0 $\pm$ 0	9 $\pm$ 7	36 $\pm$ 13	
antmaze-giant-navigate-singletask-task3-v0	0 $\pm$ 0	0 $\pm$ 0	34 $\pm$ 22	0 $\pm$ 0	0 $\pm$ 0	0 $\pm$ 0	0 $\pm$ 0	0 $\pm$ 0	0 $\pm$ 1	2 $\pm$ 3	
antmaze-giant-navigate-singletask-task4-v0	0 $\pm$ 0	0 $\pm$ 0	5 $\pm$ 12	0 $\pm$ 0	0 $\pm$ 0	0 $\pm$ 0	9 $\pm$ 4	0 $\pm$ 0	14 $\pm$ 23	5 $\pm$ 8	
antmaze-giant-navigate-singletask-task5-v0	1 $\pm$ 1	19 $\pm$ 7	49 $\pm$ 22	0 $\pm$ 1	0 $\pm$ 0	0 $\pm$ 0	6 $\pm$ 10	13 $\pm$ 9	16 $\pm$ 28	16 $\pm$ 19	
humanoidmaze-medium-navigate-singletask-task1-v0 (*)	1 $\pm$ 0	32 $\pm$ 7	16 $\pm$ 9	1 $\pm$ 1	0 $\pm$ 0	38 $\pm$ 19	6 $\pm$ 2	25 $\pm$ 8	69 $\pm$ 19	19 $\pm$ 12	21 $\pm$ 11
humanoidmaze-medium-navigate-singletask-task2-v0	1 $\pm$ 0	41 $\pm$ 9	18 $\pm$ 16	1 $\pm$ 1	1 $\pm$ 1	47 $\pm$ 35	40 $\pm$ 2	76 $\pm$ 10	85 $\pm$ 11	94 $\pm$ 3	69 $\pm$ 5
humanoidmaze-medium-navigate-singletask-task3-v0	6 $\pm$ 2	25 $\pm$ 5	36 $\pm$ 13	0 $\pm$ 1	2 $\pm$ 1	83 $\pm$ 18	19 $\pm$ 2	27 $\pm$ 11	49 $\pm$ 49	74 $\pm$ 18	63 $\pm$ 14
humanoidmaze-medium-navigate-singletask-task4-v0	0 $\pm$ 0	0 $\pm$ 1	15 $\pm$ 16	1 $\pm$ 1	1 $\pm$ 1	5 $\pm$ 4	1 $\pm$ 1	1 $\pm$ 2	1 $\pm$ 1	3 $\pm$ 4	6 $\pm$ 7
humanoidmaze-medium-navigate-singletask-task5-v0	2 $\pm$ 1	66 $\pm$ 4	24 $\pm$ 20	1 $\pm$ 1	3 $\pm$ 3	91 $\pm$ 5	31 $\pm$ 7	63 $\pm$ 9	98 $\pm$ 2	97 $\pm$ 2	81 $\pm$ 7
humanoidmaze-large-navigate-singletask-task1-v0 (*)	0 $\pm$ 0	3 $\pm$ 1	2 $\pm$ 1	0 $\pm$ 0	1 $\pm$ 1	0 $\pm$ 0	0 $\pm$ 1	6 $\pm$ 2	7 $\pm$ 6	3 $\pm$ 4	
humanoidmaze-large-navigate-singletask-task2-v0	0 $\pm$ 0	0 $\pm$ 0	0 $\pm$ 0	0 $\pm$ 0	0 $\pm$ 0	0 $\pm$ 0	0 $\pm$ 0	0 $\pm$ 0	0 $\pm$ 0	0 $\pm$ 4	
humanoidmaze-large-navigate-singletask-task3-v0	1 $\pm$ 1	7 $\pm$ 3	8 $\pm$ 4	3 $\pm$ 1	1 $\pm$ 1	2 $\pm$ 3	1 $\pm$ 1	10 $\pm$ 2	48 $\pm$ 10	11 $\pm$ 7	10 $\pm$ 6
humanoidmaze-large-navigate-singletask-task4-v0	1 $\pm$ 0	1 $\pm$ 0	1 $\pm$ 1	0 $\pm$ 0	0 $\pm$ 0	0 $\pm$ 1	0 $\pm$ 0	0 $\pm$ 0	1 $\pm$ 1	2 $\pm$ 3	8 $\pm$ 3
humanoidmaze-large-navigate-singletask-task5-v0	0 $\pm$ 1	1 $\pm$ 1	2 $\pm$ 2	0 $\pm$ 0	0 $\pm$ 0	0 $\pm$ 0	0 $\pm$ 0	1 $\pm$ 1	0 $\pm$ 0	1 $\pm$ 3	1 $\pm$ 1
antsoccer-arena-navigate-singletask-task1-v0	2 $\pm$ 1	14 $\pm$ 5	0 $\pm$ 0	44 $\pm$ 12	2 $\pm$ 1	1 $\pm$ 3	22 $\pm$ 2	17 $\pm$ 3	61 $\pm$ 25	77 $\pm$ 4	84 $\pm$ 7
antsoccer-arena-navigate-singletask-task2-v0	2 $\pm$ 2	17 $\pm$ 7	0 $\pm$ 1	15 $\pm$ 12	3 $\pm$ 1	0 $\pm$ 0	8 $\pm$ 1	8 $\pm$ 2	75 $\pm$ 3	88 $\pm$ 3	89 $\pm$ 4
antsoccer-arena-navigate-singletask-task3-v0	0 $\pm$ 0	6 $\pm$ 4	0 $\pm$ 0	0 $\pm$ 0	0 $\pm$ 0	8 $\pm$ 19	11 $\pm$ 5	16 $\pm$ 3	14 $\pm$ 22	61 $\pm$ 6	56 $\pm$ 7
antsoccer-arena-navigate-singletask-task4-v0 (*)	1 $\pm$ 0	3 $\pm$ 2	0 $\pm$ 0	0 $\pm$ 1	0 $\pm$ 0	0 $\pm$ 0	12 $\pm$ 3	24 $\pm$ 4	16 $\pm$ 9	39 $\pm$ 6	43 $\pm$ 5
antsoccer-arena-navigate-singletask-task5-v0	0 $\pm$ 0	2 $\pm$ 2	0 $\pm$ 0	0 $\pm$ 0	0 $\pm$ 0	0 $\pm$ 0	9 $\pm$ 2	15 $\pm$ 4	0 $\pm$ 1	36 $\pm$ 9	39 $\pm$ 9
cube-single-play-singletask-task1-v0	10 $\pm$ 5	88 $\pm$ 3	89 $\pm$ 5	95 $\pm$ 2	89 $\pm$ 7	77 $\pm$ 28	81 $\pm$ 9	73 $\pm$ 33	79 $\pm$ 4	97 $\pm$ 2	96 $\pm$ 3
cube-single-play-singletask-task2-v0 (*)	3 $\pm$ 1	85 $\pm$ 8	92 $\pm$ 4	96 $\pm$ 2	82 $\pm$ 16	80 $\pm$ 30	81 $\pm$ 9	83 $\pm$ 13	73 $\pm$ 3	97 $\pm$ 2	99 $\pm$ 1
cube-single-play-singletask-task3-v0	9 $\pm$ 3	91 $\pm$ 5	93 $\pm$ 3	99 $\pm$ 1	96 $\pm$ 2	98 $\pm$ 1	87 $\pm$ 4	82 $\pm$ 12	88 $\pm$ 4	98 $\pm$ 2	100 $\pm$ 1
cube-single-play-singletask-task4-v0	2 $\pm$ 1	73 $\pm$ 6	92 $\pm$ 3	93 $\pm$ 4	70 $\pm$ 18	91 $\pm$ 2	79 $\pm$ 6	79 $\pm$ 20	79 $\pm$ 6	94 $\pm$ 3	95 $\pm$ 4
cube-single-play-singletask-task5-v0	3 $\pm$ 3	78 $\pm$ 9	87 $\pm$ 8	90 $\pm$ 6	61 $\pm$ 12	80 $\pm$ 20	78 $\pm$ 10	76 $\pm$ 33	77 $\pm$ 7	93 $\pm$ 3	92 $\pm$ 5
cube-double-play-singletask-task1-v0	8 $\pm$ 3	27 $\pm$ 5	45 $\pm$ 6	39 $\pm$ 19	7 $\pm$ 6	21 $\pm$ 8	21 $\pm$ 7	47 $\pm$ 11	35 $\pm$ 9	61 $\pm$ 9	65 $\pm$ 6
cube-double-play-singletask-task2-v0 (*)	0 $\pm$ 0	1 $\pm$ 1	7 $\pm$ 3	16 $\pm$ 10	0 $\pm$ 0	2 $\pm$ 2	2 $\pm$ 1	22 $\pm$ 12	9 $\pm$ 5	36 $\pm$ 6	49 $\pm$ 13
cube-double-play-singletask-task3-v0	0 $\pm$ 0	0 $\pm$ 0	4 $\pm$ 1	17 $\pm$ 8	0 $\pm$ 1	3 $\pm$ 1	1 $\pm$ 1	4 $\pm$ 2	8 $\pm$ 5	22 $\pm$ 5	34 $\pm$ 15
cube-double-play-singletask-task4-v0	0 $\pm$ 0	0 $\pm$ 0	1 $\pm$ 1	0 $\pm$ 1	0 $\pm$ 0	0 $\pm$ 1	0 $\pm$ 0	0 $\pm$ 1	1 $\pm$ 1	5 $\pm$ 2	7 $\pm$ 4
cube-double-play-singletask-task5-v0	0 $\pm$ 0	4 $\pm$ 3	4 $\pm$ 2	1 $\pm$ 1	0 $\pm$ 0	3 $\pm$ 2	2 $\pm$ 1	2 $\pm$ 2	17 $\pm$ 6	19 $\pm$ 10	46 $\pm$ 11
scene-play-singletask-task1-v0	19 $\pm$ 6	94 $\pm$ 3	95 $\pm$ 2	100 $\pm$ 0	94 $\pm$ 4	100 $\pm$ 1	87 $\pm$ 8	96 $\pm$ 8	98 $\pm$ 3	100 $\pm$ 0	98 $\pm$ 2
scene-play-singletask-task2-v0 (*)	1 $\pm$ 1	12 $\pm$ 3	50 $\pm$ 13	33 $\pm$ 14	2 $\pm$ 2	50 $\pm$ 40	18 $\pm$ 8	46 $\pm$ 10	0 $\pm$ 0	76 $\pm$ 9	59 $\pm$ 17
scene-play-singletask-task3-v0	1 $\pm$ 1	32 $\pm$ 7	55 $\pm$ 16	94 $\pm$ 4	4 $\pm$ 4	49 $\pm$ 16	38 $\pm$ 9	78 $\pm$ 14	54 $\pm$ 19	98 $\pm$ 1	85 $\pm$ 5
scene-play-singletask-task4-v0	2 $\pm$ 2	0 $\pm$ 1	3 $\pm$ 3	4 $\pm$ 3	0 $\pm$ 0	0 $\pm$ 0	6 $\pm$ 1	4 $\pm$ 4	0 $\pm$ 0	5 $\pm$ 1	13 $\pm$ 8
scene-play-singletask-task5-v0	0 $\pm$ 0	0 $\pm$ 0	0 $\pm$ 0	0 $\pm$ 0	0 $\pm$ 0	0 $\pm$ 0	0 $\pm$ 0	0 $\pm$ 0	0 $\pm$ 0	0 $\pm$ 0	0 $\pm$ 0
puzzle-3x3-play-singletask-task1-v0	5 $\pm$ 2	33 $\pm$ 6	97 $\pm$ 4	52 $\pm$ 12	89 $\pm$ 5	97 $\pm$ 2	25 $\pm$ 9	63 $\pm$ 19	94 $\pm$ 3	90 $\pm$ 4	89 $\pm$ 7
puzzle-3x3-play-singletask-task2-v0	1 $\pm$ 1	4 $\pm$ 3	1 $\pm$ 1	0 $\pm$ 1	0 $\pm$ 1	0 $\pm$ 0	4 $\pm$ 2	2 $\pm$ 2	1 $\pm$ 2	16 $\pm$ 5	38 $\pm$ 11
puzzle-3x3-play-singletask-task3-v0	1 $\pm$ 1	3 $\pm$ 2	3 $\pm$ 1	0 $\pm$ 0	0 $\pm$ 0	0 $\pm$ 0	1 $\pm$ 0	1 $\pm$ 1	0 $\pm$ 0	10 $\pm$ 3	35 $\pm$ 11
puzzle-3x3-play-singletask-task4-v0 (*)	1 $\pm$ 1	2 $\pm$ 1	2 $\pm$ 1	0 $\pm$ 0	0 $\pm$ 0	0 $\pm$ 0	1 $\pm$ 1	2 $\pm$ 2	0 $\pm$ 0	16 $\pm$ 5	23 $\pm$ 8
puzzle-3x3-play-singletask-task5-v0	1 $\pm$ 0	3 $\pm$ 2	5 $\pm$ 3	0 $\pm$ 0	0 $\pm$ 0	0 $\pm$ 0	1 $\pm$ 1	2 $\pm$ 2	0 $\pm$ 0	16 $\pm$ 3	31 $\pm$ 8
puzzle-4x4-play-singletask-task1-v0	1 $\pm$ 1	12 $\pm$ 2	26 $\pm$ 4	48 $\pm$ 5	24 $\pm$ 9	44 $\pm$ 10	1 $\pm$ 2	32 $\pm$ 9	49 $\pm$ 9	34 $\pm$ 8	23 $\pm$ 3
puzzle-4x4-play-singletask-task2-v0	0 $\pm$ 0	7 $\pm$ 4	12 $\pm$ 4	14 $\pm$ 5	0 $\pm$ 1	0 $\pm$ 0	0 $\pm$ 1	5 $\pm$ 3	4 $\pm$ 4	16 $\pm$ 5	9 $\pm$ 2
puzzle-4x4-play-singletask-task3-v0	0 $\pm$ 0	9 $\pm$ 3	15 $\pm$ 3	34 $\pm$ 5	21 $\pm$ 10	29 $\pm$ 12	1 $\pm$ 1	20 $\pm$ 10	50 $\pm$ 14	18 $\pm$ 5	9 $\pm$ 4
puzzle-4x4-play-singletask-task4-v0 (*)	0 $\pm$ 0	5 $\pm$ 2	10 $\pm$ 3	26 $\pm$ 4	7 $\pm$ 4	1 $\pm$ 1	0 $\pm$ 0	5 $\pm$ 1	21 $\pm$ 11	11 $\pm$ 3	7 $\pm$ 4
puzzle-4x4-play-singletask-task5-v0	0 $\pm$ 0	4 $\pm$ 1	7 $\pm$ 3	24 $\pm$ 11	1 $\pm$ 1	0 $\pm$ 0	0 $\pm$ 1	4 $\pm$ 3	2 $\pm$ 2	7 $\pm$ 3	7 $\pm$ 4
antmaze-umaze-v2	55	77	98	94	97	66 $\pm$ 5	90 $\pm$ 6	94 $\pm$ 3	92 $\pm$ 6	96 $\pm$ 2	96 $\pm$ 3
antmaze-umaze-diverse-v2	47	54	84	80	82	66 $\pm$ 11	55 $\pm$ 7	82 $\pm$ 9	62 $\pm$ 12	89 $\pm$ 5	87 $\pm$ 8
antmaze-medium-play-v2	0	66	90	84	81	49 $\pm$ 24	52 $\pm$ 12	77 $\pm$ 7	56 $\pm$ 15	78 $\pm$ 7	80 $\pm$ 7
antmaze-medium-diverse-v2	1	74	84	85	75	0 $\pm$ 1	44 $\pm$ 15	77 $\pm$ 6	60 $\pm$ 25	71 $\pm$ 13	76 $\pm$ 19
antmaze-large-play-v2	0	42	52	64	54	0 $\pm$ 0	10 $\pm$ 6	32 $\pm$ 21	55 $\pm$ 9	84 $\pm$ 7	78 $\pm$ 6
antmaze-large-diverse-v2	0	30	64	68	54	0 $\pm$ 0	16 $\pm$ 10	20 $\pm$ 17	64 $\pm$ 8	83 $\pm$ 4	78 $\pm$ 6
pen-human-v1	71	78	103	76 $\pm$ 10	69 $\pm$ 7	64 $\pm$ 8	67 $\pm$ 5	77 $\pm$ 7	71 $\pm$ 12	53 $\pm$ 6	61 $\pm$ 9
pen-cloned-v1	52	83	103	64 $\pm$ 7	61 $\$						